Evaluation of the precision and accuracy of the QUB/e method for assessing the as-built thermal performance of a low-energy detached house in UK

Johann Meulemans, Vasileios Sougkakis, Christopher Wood, Mark Gillott, Tom Cox

Energy & Buildings (2021) 111643, https://doi.org/10.1016/j.enbuild.2021.111643

Evaluation of the precision and accuracy of the QUB/e method for assessing the as-built thermal performance of a low-energy detached house in UK

Vasileios Sougkakis[1,2], Johann Meulemans*[3], Christopher Wood[1], Mark Gillott[1], and Tom Cox[2]

[1]The University of Nottingham, University Park, Nottingham, NG7 2RD, UK
[2]Saint-Gobain UK & Ireland, East Leake, Leicestershire, LE12 6HX, UK
[3]Saint-Gobain Research Paris, 39 quai Lucien Lefranc, F-93303 Aubervilliers, France

October 11, 2021

Abstract

In this paper, the findings from a field study of the thermal performance of a low-energy dwelling are presented and discussed. The study aimed at evaluating the precision and accuracy of the QUB/e method in the field under UK climatic conditions. A series of in situ measurements were carried out in a low-energy detached house located in the University Park campus, University of Nottingham to determine both the whole building Heat Transfer Coefficient (HTC) and the thermal transmittances (U-values) of the external walls and the glazings. The values determined with well-established quasi-static measurement methods (coheating test, ISO 9869-1 average method) were used as reference (benchmark) values to assess the accuracy of the QUB/e method. In total 18 consecutive QUB/e tests were conducted.

The QUB/e method was able to provide precise and accurate estimates of the whole building HTC: 94% of the results (i.e. 17 out of 18) were found to be within ± 15% from the mean and 78% of the HTC estimates (i.e., 14 out of 18) obtained with a QUB/e test could not be considered statistically different from the HTC determined with the coheating test (benchmark). It should be noted that the reported confidence intervals associated with the HTC estimates obtained with the QUB/e tests were slightly larger than the one reported for the coheating test (i.e., 11.6% in average and 6.1%, respectively). The Mean Bias Error (MBE) and the Root Mean Square Error (RMSE) associated with the HTC estimates obtained with the QUB/e tests were approximately 11%.

The QUB/e method was also able to provide precise and accurate estimates of the thermal transmittances of the external walls and the glazings. We observed that all but seven (i.e., 119 out of 126 or 94%) U-values estimates of the external walls obtained with a QUB/e test could not be considered statistically different from the U-values determined with the ISO 9869-1 average method (benchmark). With regard to the glazings, this was observed for all U-values estimates (i.e., 162 out of 162 or 100%). It should be noted that the reported confidence intervals associated with the U-value estimates obtained with both test methods were close (i.e., approximately 10% in average) for all elements except for the ICF wall.

Keywords— QUB/e method; heat transfer coefficient; U-value; in situ measurements

*corresponding author: johann.meulemans@saint-gobain.com

1 Introduction

Building regulations in the UK have been setting progressively stricter requirements over recent years in relation to the energy efficiency of new-built dwellings. This has been done in order to reduce greenhouse gas emissions from the domestic sector, which currently accounts for 29.5% of the country's final energy consumption [1]. However, it has been found that the design thermal performance is often inconsistent with the actual as-built thermal performance of a dwelling. This difference is commonly referred to as the 'performance gap' (e.g., see [2–4] and references therein) and is considered a significant risk that not only undermines the effectiveness of building regulations and the efforts on reducing greenhouse gas emissions but may also have detrimental effect on the reputation of the house building industry [5, 6].

Addressing this gap is therefore considered a matter of utmost importance and to do so there is the requirement of applying robust methodologies to determine both the design and the as-built performance of buildings. For this reason, a metric is used to assess specifically the performance of the building fabric and the quality of the construction (isolating any effects of the occupant behavior when determining the performance gap), the Heat Transfer Coefficient (HTC) [7]. The HTC is an indicator that accounts for both the transmission losses occurring through the building elements (including thermal bridges) and the infiltration losses of the building envelope. The HTC is a global parameter that represents the heat losses from the whole building per degree of temperature difference between the internal and external environment and is measured in $\mathrm{W\,K^{-1}}$.

Calculating the design HTC of a dwelling is part of the regulatory process using the UK Government's Standard Assessment Procedure (SAP) and is based on information of the building geometry, location, surroundings and material properties [8]. In contrast, assessing the as-built performance is not as simple and straightforward.

With regard to the whole building thermal performance, several methods have been developed to determine the actual HTC of the building fabric in situ (e.g., coheating [9, 10], PRISM [11], PSTAR [12], QUB [13] and ISABELE [14]). Perhaps the most widely used of these methods is the coheating test, a quasi-steady state method that determines the HTC of a building by maintaining a fixed internal elevated temperature using heaters and fans for a significant period of time (typically 2–4 weeks) and monitoring the power required to do so as well as the external temperature and weather conditions. There is no standardised method for conducting the test, however the vast majority of coheating tests are now performed according to the protocol developed by Leeds Metropolitan University (now Leeds Beckett University) [15].

With regard to the elemental performance, the thermal transmittance (or the thermal resistance) of building elements is commonly measured in situ with the use of the Heat Flow Meter (HFM) method [16]. BS ISO 9869-1:2014 standard describes the recommended procedure for determining the U-value of building elements in situ with the use of the HFM method. The 'average method' described in the standard is the most widely used analysis technique. This method considers measuring the heat flow at the surface of a building element and temperatures at each side of that element and averaging them over long periods of time so that heat storage effects are minimised (i.e., quasi-steady state conditions are assumed); likewise, long testing periods are usually required in order to meet the criteria set by the average method. BS ISO 9869-1:2014 also includes a 'dynamic method' to evaluate the thermal transmittance of building elements under transient conditions, however it is not commonly used due to its increased complexity.

Both the coheating and the HFM methods are not considered practical by industry as they involve long testing periods when the occupants are required to leave their property and are restricted during the heating season when the external temperature and the levels of solar radiation are typically low. The scope for more practical, less time and resources consuming alternatives that could be applied for quality assurance purposes has been highlighted as early as 2011 when it was included in the recommendations of the Good Homes Alliance Monitoring Programme report [17].

Several in situ measurement methods have been recently developed and/or improved to assess the as-built HTC of buildings (e.g., see work carried out within IEA EBC Annex 58 on dynamic methods [18] and then further developed within IEA EBC Annex 71 (e.g., see [19,20])). Recent comprehensive reviews of experimental measurement methods available to estimate the thermal transmittance (or thermal resistance) of building elements based on contact or non contact measurements can be found in [21–23]. The description of these different experimental techniques falls outside the scope of the present paper. The interested reader can refer to the above cited reviews.

The QUB/e method [24] is an in situ dynamic measurement method developed to determine the as-built HTC of dwellings and the thermal transmittances (U-values) of building elements within one night without occupancy. The QUB/e method builds on the QUB method. Based on the same analysis principle, the QUB/e method takes into account the heat flow on building elements to determine the U-values. A distinctive advantage of the QUB/e method is the time required to carry out a measurement: a single night for a test compared to an average duration of 2 to 4 weeks for a coheating test (for the HTC) or HFM (for the U-values).

The ability of the QUB method to provide reliable results, has been demonstrated numerically [13, 25, 26] and experimentally in a climate chamber under steady conditions [13,24,27]. Several studies have also reported

on the precision and accuracy of the method under actual climatic conditions in different regions of Europe (e.g., see [13, 24, 28–31]). These studies highlighted the ability of the method to provide reliable results and its applicability as a research tool.

In this paper, results from the second part of a two-year field testing campaign are presented where a series of QUB/e tests were performed on a daily basis in a well-insulated property in the UK climate in order to examine the precision and accuracy of the method in a building with high levels of energy efficiency similar to those of new-built dwellings. The measured values determined with a coheating test (HTC) and the HFM method (U-values) were considered as the reference (benchmark) values to assess the accuracy of the QUB/e method.

2 In situ measurement methods

2.1 Coheating test

The method statement for the coheating test is described in [15]. The test procedure involves heating the building with electrical heaters to a fixed elevated temperature, significantly higher than the mean external temperature (usually 25 °C) so that an adequate temperature difference between internal and external environment is achieved. Fans are used to mix the air and achieve homogeneous temperatures throughout the building. Internal zone temperatures, the external temperature and the energy consumption of the fans and heaters are monitored. The test is conducted in an unoccupied building and any electrical appliances are switched off so that there are no other internal heat gains that are not accounted for. The method is based on the building's energy balance where the heat gains are equal to the heat losses. In order for this assumption to hold true, any transient effects of heat stored in the building fabric should be diminished. Quasi steady-state conditions are assumed and to achieve this the building is constantly heated to maintain the elevated internal temperature for a period of time. As the external conditions are not steady-state, the data are aggregated on a 24-hour basis in order to average and minimise the effect of dynamic heat flows. The energy balance considered during a coheating test is described by Equations 1 to 3.

$$Q_{elec} + Q_{solar} = Q_{loss} \tag{1}$$

$$Q_{elec} + Q_{solar} = H\Delta T \tag{2}$$

$$Q_{elec} + GS = H\Delta T \tag{3}$$

Q_{elec} and Q_{solar} are the power consumption of the electrical heaters (in W) and the solar gains (in W), respectively. Collectively, these two terms are the heat gains of the building during the test, as due to the test protocol there are no other internal gains in the building. Q_{loss} is the rate of heat loss of the dwelling (in W). This is the product of the HTC, H (in $W\,K^{-1}$), and the temperature difference between the average internal and average external temperatures, ΔT (in K). Solar gains can be accounted for by measuring the solar irradiance, S (in $W\,m^{-2}$), using a pyranometer and calculating the solar aperture, G (in m^2) [15,36].

There are two main methods to determine the HTC and consequently the solar aperture, G. Either through linear regression where the power consumption of the electrical heaters is the dependent variable and the temperature difference between internal and external environment and the solar irradiance are the independent variables or with the 'Siviour method' where Equation 3 is rearranged as follows:

$$\frac{Q_{elec}}{\Delta T} = H - G\frac{S}{\Delta T} \tag{4}$$

The HTC is then determined by plotting a graph of the daily average values of the $Q_{elec}/\Delta T$ at the y-axis and the $S/\Delta T$ at the x-axis and fitting a regression line. The HTC is the intercept of the line at the y-axis and the solar aperture, G, is the slope of the line [15]. A review of other analysis techniques for obtaining the HTC and the solar aperture can be found in [37, 38] and references therein but these will not be discussed here as they fall outside the scope of this work.

There is no specific requirement on the duration of the test, however Johnston et al. [15] suggested that typically 1-3 weeks is required after a building has been thermally saturated (i.e. reached quasi-steady state conditions) depending on the construction type and the weather conditions. Stamp [36] reported on duration of published tests varying from 6 to 32 days.

2.2 Heat Flow Meter (HFM) method (ISO 9869-1)

BS ISO 9869-1:2014 describes the procedure for determining the thermal transmittance (U-value) of building elements in situ with the use of heat flow meters. The average method is based on the assumption that after

a significant amount of time, the average values of temperature and density of heat flow rate are approaching steady-state conditions [16]. The U-value is determined by dividing the mean heat flux through a building element by the mean temperature difference between the internal and external side of that element over a long period of time (Equation 5).

$$U = \frac{\sum_{j=1}^{n} q_j}{\sum_{j=1}^{n} (T_{int,j} - T_{ext,j})} \tag{5}$$

U is the thermal transmittance of the building element (in $W\,m^{-2}$), q_j is density of heat flow rate at time step j (in $W\,m^{-2}\,K^{-1}$) and $T_{int,j}$ and $T_{ext,j}$ are the internal and external environmental temperature respectively at time step j (in K). In practice, when both internal and external temperatures fluctuate on a daily basis, it may be difficult for these criteria to be met which may result in significantly long testing periods. However, when this method is applied when a coheating test is performed (i.e. internal temperature remains stable), the required testing period to meet the criteria is reduced [40]. In any case, the minimum (normative) test duration is three days for the most favourable conditions and lightweight elements.

The duration of the test is determined by specific criteria that have been set to assume quasi-static conditions are met. The test is completed once the thermal resistance value (R-value) obtained over different sub-periods of the whole test period does not deviate more than ±5%. For lightweight elements it is recommended that only data obtained at night time are used and the test is completed when the resistance values do not differ by more than ±5% for three consecutive nights. For heavyweight elements more stringent requirements have been set in order to account for thermal storage phenomena. The period required is an integer multiple of 24 hours with a minimum test duration of 72 hours. In addition the R-value at the end of the test should not deviate more than ±5% from that obtained 24 hours earlier and the R-value obtained at the first two-thirds of the test period should not deviate by more than ±5% from that obtained at the last two thirds [16].

2.3 QUB/e method

The QUB method was developed to determine the as-built HTC of dwellings within one night without occupancy. The test commences after sunset and finishes before sunrise of the following day (Figure 1b). The principle of the QUB method is based on a single resistance and capacitance model [13] where the building is represented by a global thermal resistance R (the reciprocal of the HTC of the building) and a global capacitance, C (the internal heat capacity) (Figure 1a). Internal and external temperature nodes (T_{int} and T_{ext} respectively) are considered homogeneous and heat exchange between the two nodes occurs through the thermal resistance, R. Temperature evolution is described as a single decaying exponential.

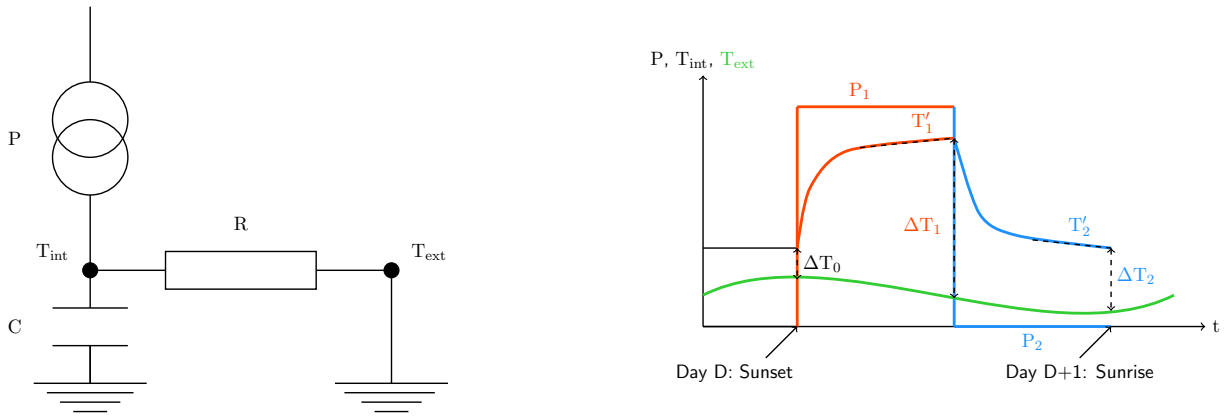

(a) RC model

(b) Evolution of power and temperatures

Figure 1: Schematic view of the QUB method

It is acknowledged that this model is crude and in reality the thermal behaviour of the envelope is much more complex. A more detailed representation would involve a larger RC network with more nodes and, hence, more time constants. The thermal response of the building in that case would be the superposition of a number of decaying exponentials. However, it has been shown that after a sufficient amount of time the single RC model provides a good approximation of the building conditions and the model becomes valid [13, 25]. Based on the

single RC model, the energy input, P, is heat lost through the envelope and stored/released by the thermal mass of the fabric (Equation 6):

$$P = \frac{T_{int} - T_{ext}}{R} + C\frac{dT_{int}}{dt} \tag{6}$$

Where, P is the power input (in W) in the building, T_{int} and T_{ext} are the internal and outside temperature (in K) respectively, R is the global resistance (in $K\,W^{-1}$) of the building (the reciprocal of the HTC that accounts for the transmission and infiltration losses) and C is the apparent heat capacitance (in $J\,K^{-1}$) of the envelope.

Equation 6 involves two unknowns, R and C. These can then be determined by using two different constant powers in two different phases of equal duration (respectively noted 1 and 2 in Figure 1b) and solving a system of two equations. The HTC, noted H, can then be derived by the following formula (Equation 7):

$$H = \frac{T'_2 P_1 - T'_1 P_2}{T'_2 \Delta T_1 - T'_1 \Delta T_2} \tag{7}$$

Where P_i is the power input during phase i, T'_i is the slope of the temperature profile at the end of phase i (i.e., for $t \in [t_{i_0} + d_i - \min(d_i/2, \tau), t_{i_0} + d_i]$ where t_{i_0} is the beginning of phase i, d_i the duration of phase i and $\tau = 2\,h$) and ΔT_i is the internal to external temperature difference at the end of phase i [24].

It is apparent that for an accurate measurement of the HTC, there needs to be an accurate measurement of the power input, P. To do this and avoid unwanted heat gains that are difficult to quantify (such as solar gains, metabolic heat gains from occupants etc.) the test is carried at night in an empty unoccupied dwelling without additional heat sources. To simplify matters there is no power input in phase 2 ($P_2 = 0\,W$), i.e. this is the free cooling phase.

Further development of the method involved the use of a quadrupole model based on the same assumptions to investigate the thermal response of the building in short duration. A detailed description of the model is given by Alzetto et al. [13]. This approach led to establishing specific criteria considering the testing conditions with regard to the power input and the internal and external temperature that, when met, allow for a reliable measurement to take place. These criteria have been summed to a dimensionless parameter inherent to the QUB method, the α-parameter, α (e.g., see [13] and references therein) (Equation 8).

$$\alpha = 1 - \frac{H_{ref}\Delta T_0}{P_1} \tag{8}$$

Where H_{ref} is a reference HTC (theoretical or determined experimentally) (in $W\,K^{-1}$), ΔT_0 is the initial temperature difference between the internal and the external environment (in K) and P_1 is the power input during the heating phase (in W).

It has been demonstrated that the α-parameter has minimum effect on the resulting HTC for values $0.4 \leq \alpha \leq 0.7$, while for $\alpha \geq 0.7$ there is usually an overestimation of the HTC mostly at very short tests [24, 28]. Hence, meeting this criterion is considered a measure of confidence level for test accuracy.

With the QUB/e method [24,30], heat flux densities and nearby air temperatures for each building element of interest are monitored during a QUB test. The QUB analysis procedure is then used to derive the U-values of each building element, noted U:

$$U = \frac{T'_2 q_1 - T'_1 q_2}{T'_2 \Delta T_1 - T'_1 \Delta T_2} \tag{9}$$

Where q_i, T'_i, and ΔT_i are the mean heat flux density (in $W\,m^{-2}$), the slope of the temperature profile, and the internal to external temperature difference at the end of phase i (i.e., for $t \in [t_{i_0} + d_i - \min(d_i/2, \tau), t_{i_0} + d_i]$ where t_{i_0} is the beginning of phase i, d_i the duration of phase i and $\tau = 2\,h$) [24], respectively.

The Taylor series method for uncertainty propagation [41] is used to compute the relative expanded uncertainties (95% confidence interval) associated with the estimates of the HTC and the U-values.

The whole HTC and the local U-values of a building can thus be estimated in one night using the QUB/e method. For more details on the QUB/e method and previous work, the interested reader should refer to [13, 24, 30] and references therein.

3 Field testing campaign

3.1 Description of the house

The tests were carried in a two-storey detached house located at 6, Green Close, at the Creative Energy Homes site at the University of Nottingham Park Campus. The house was completed in 2008 and achieved level 4 of

the UK's Code for Sustainable Homes [32]. The design of the house considered a fabric first approach. The walls and roof had a design U-value of 0.15 $W\,m^2\,K^{-1}$ and the floor 0.14 $W\,m^2\,K^{-1}$. The ground floor walls were built with Insulating Concrete Formwork (ICF) construction and the first floor walls and roof were constructed with timber Structural Insulated Panels (SIPs). The south façade is a sunspace with internal and external fully glazed surfaces. The North wall has small windows while the East and West walls do not have any windows. The windows are double glazed with design U-values of 1.66 and 1.70 $W\,m^{-2}\ K^{-1}$ for the north façade and the south façade, respectively [33]. The house has North orientation. The internal volume of the house is 285 m^3 and the internal envelope area, i.e. the area of walls, floor and ceiling enclosing the heated space and separating it from the external environment is about 290 m^2 [34]. The building's total heated floor area is approximately 100 m^2 [35]. All measurements refer to the internal side of the building envelope disregarding any internal partition walls and floors as suggested by the Standard Assessment Procedure (SAP) [8]. The plans and an external view of the house are shown in Figure 2 and Figure 3, respectively.

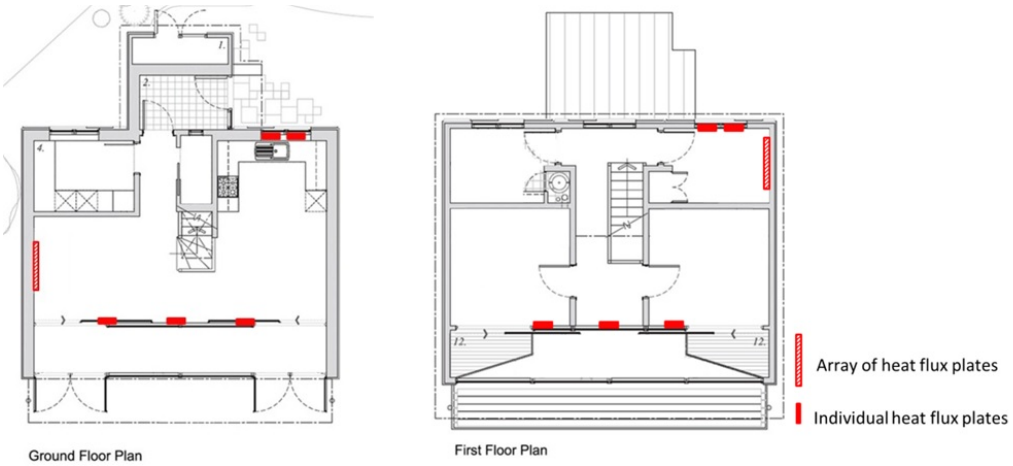

Figure 2: Ground floor (left) and first floor plan (right) of the test house and location of heat flux sensors

Figure 3: External view of the house

3.2 Monitoring equipment and testing protocol

In order to perform the quasi-static and dynamic tests the following parameters were required to be monitored: internal ambient temperatures in the different zones, external air temperature, heat flux density at the surface of the building elements, temperature at the vicinity of these elements and power input. During the coheating test, temperatures at the different locations were measured with the use of Platinum RTD sensors (PT100) and the heat flux density was measured with the use of Hukseflux HFP01 heat flux plates. Heat flux sensors were installed on the ground and first floor walls (an array of heat flux sensors was installed in each wall area to obtain an average U-value), the external windows and the internal sunspace windows as shown in Figure 2. The

energy consumed by the heaters was monitored by energy meters that produce a pulse for every Wh measured. Data were stored in two Datataker DT85 loggers with two CEM-20 expansion modules and were recorded at 1 minute intervals. The same equipment was used during the QUB/e measurements so that results compared were obtained under the same conditions. Two Skye SKS-1110 pyranometers were installed externally in the south façade in order to obtain an average measurement of the south facing vertical solar irradiance. This was then used to account for the solar gains in the resulting HTC. Weather conditions were recorded with a WSD1 sensor by EML and a Skye rht+ sensor that was installed in a neighbouring property.

During the coheating test, electric resistance fan heaters with three power settings (650 W, 1300 W and 2000 W) were used throughout the house. The heaters were controlled by PID thermostatic controllers with PT100 sensors that were set to maintain the internal temperature at 25 °C. Fans were used to mix the air inside the building as per the method statement described in [15]. The QUB/e tests were conducted without the use of fans. Instead temperature homogeneity was achieved with the use of several fan heaters spread throughout the house and arranging the power according to the room volumes. Two different types of fan heaters were used for flexibility in the distribution of power; a set of 2 kW electric fan heaters similar to the ones used in the coheating test and another set of heaters with lower power ratings (two settings at 170 W and 250 W). Apart from distributing the heat input evenly throughout the house, the different types of heaters also allowed for adjustments in the total power to be made according to the expected external temperature for each test in order to keep the α-parameter within the recommended limits (between 0.4 and 0.7). With regard to the α-parameter calculation, the HTC determined with the coheating test was used as the reference HTC. In total, 18 consecutive QUB/e tests were analysed. Duration of the tests was between 12-14 hours (i.e. heating/cooling phase duration between 6-7 hours). It has been shown that such duration is adequate to obtain results that are not affected by the α-parameter [24, 28].

The schedule for each set of measurements is presented in Table 1 below.

Method(s)	Period	No. of tests
Quasi-static measurements (coheating, ISO 9869-1)	04/11/2017 – 26/11/2017	1
Dynamic measurements (QUB/e)	28/11/2017 – 17/12/2017	18

Table 1: Testing schedule of the quasi-static and dynamic measurements

The coheating test was conducted in November 2017 over a period of 23 days. As the south façade had such a large area of glazing, special consideration had to be given to minimise the effect of solar gains through the sunspace. It was considered that the dwelling could be subject to great swings in solar gains, and at times of high solar radiation, this heat gain could dominate the heat input to the dwelling, which may lead to difficulties maintaining the internal fixed temperature and increase the test uncertainty. It was therefore decided in order to mitigate this effect that the blinds in the external glazing of the sunspace would be kept closed while windows that did not have blinds would be covered with aluminum foil to reflect incoming radiation. In addition, the top windows were left open (Figure 4).

Figure 4: External view of the south façade of the dwelling with the location of the pyranometers. Most glazed areas were covered to minimise the effect of solar radiation.

Therefore, the heated area of the house did not include the sunspace. This arrangement was very effective

at allowing full control of the internal conditions; there were no incidents of solar gains resulting in internal temperatures higher than the 25 °C setpoint. This can be seen in Figure 5a where homogeneous temperatures throughout the different zones of the house were achieved and the temperature setpoint was never exceeded throughout a 24-hour period. This arrangement was kept the same throughout the whole course of the quasi-static and dynamic measurements. The temperature and power profile during a typical QUB/e test is shown in Figure 5b.

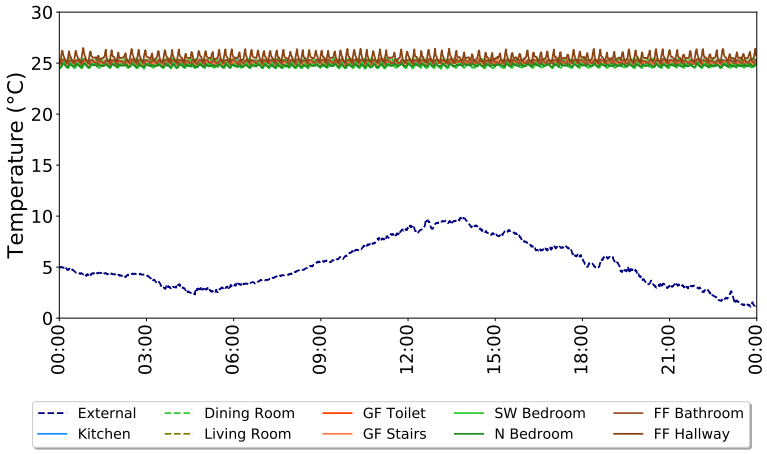

(a) 05/11/2017 - Coheating

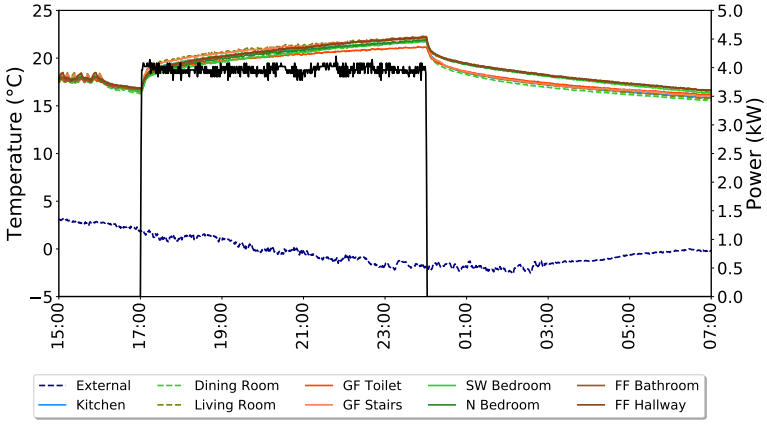

(b) 16-17/12/2017 – QUB/e test no. 18

Figure 5: Evolution of power and temperatures during the coheating test and a typical QUB/e test

3.3 Heat transfer coefficient measurements – Coheating analysis

To determine the HTC of the house, recorded data of ambient temperatures (internal and external), power consumption of heaters and south vertical solar radiation were averaged on a daily basis. This resulted in obtaining 22 data points for the analysis during the coheating test. It should be noted that one data point from a day with significantly higher average wind speed than any other day and significantly higher power consumption on that day was treated as an outlier and was omitted from the analysis so that it would not affect the regression [42]. In order to smooth the effects of thermal storage during the coheating test, a Multiple Linear Regression (MLR) analysis is presented in Figure 6. The south vertical irradiation data were aggregated from 06:00 am until 05:59 am the following morning in order to allow for solar gains to be readmitted back to space [15, 43]. The south vertical irradiance measured was used as the independent variable. For better visualisation in a 2-D diagram, the solar aperture calculated by the MLR analysis was multiplied by the daily average solar irradiance measured to determine the average daily solar gains. These gains were then added to the average daily power consumed by the heaters, i.e. the y-axis of Figure 6 represents the sum of electrical power and the solar gains (Q_{elec} and Q_{solar} in Equation 1). MLR analysis in general has been reported as statistically better in correcting the HTC for solar gains than the Siviour analysis since it considers both solar irradiance, S, and the temperature difference ΔT as independent variables [44]. Bauwens and Roels [37] also recommended the use of MLR analysis as the Siviour analysis may lead to unreliable results when ΔT is close

to 0 K. However, the test protocol considers a minimum ΔT of 10 K and it has been shown in literature that both methods result in very similar estimates of the HTC [36].

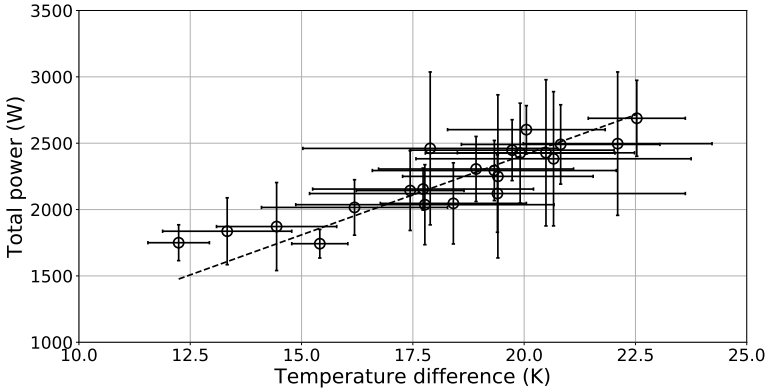

Figure 6: Multiple Linear Regression (MLR) analysis of the coheating test data

The HTC was found to be 120.6 ± 7.3 W K^{-1} (95% confidence interval) when using the MLR analysis (see Figure 6). For reasons of comparison, it should be mentioned that the Siviour analysis resulted to a HTC of 122.5 ± 8.0 W K^{-1} (95% confidence interval) which is consistent with the literature findings suggesting that the two methods lead to very similar results. The relative uncertainties are consistent with the values reported by Jack et al. [39]. The value of the HTC determined with the MLR analysis will be used in the remainder of the paper.

3.4 Thermal transmittance measurements

To determine the elemental performance, heat flux sensors were installed on the interior surface of the external walls, the external window panes and the internal glazing of the sunspace in each floor. The U-values were then calculated considering the procedure set by BS ISO 9869-1:2014 and the QUB/e analysis (see Equation 4 and Equation 7, respectively). As mentioned earlier, the ground floor wall construction is Insulated Concrete Formwork (ICF) and the first floor walls are of Structural Insulated Panels (SIPs). The specific heat capacity per unit area for both these constructions has been calculated using the method described in Table 1e of the Government's Standard Assessment Procedure for Energy Rating of Dwellings (2012 edition) [8] at 9 kJ m^{-2} K^{-1}. This is well below the 20 kJ m^{-2} K^{-1} threshold set in the BS ISO 9869-1:2014 for lightweight elements. Based on the recommendations of the ISO 9869-1 standard, the U-value calculation for lightweight elements should be conducted from data obtained at night and the analysis should be concluded when results from three consecutive nights are within ±5% from each other. However, it was not possible to achieve such convergence for three consecutive nights in the case of the ICF walls. The thermal behaviour of ICF construction has been the subject of several studies which highlighted that the thermal mass of the concrete in the core of the ICF construction is not thermally decoupled from the internal conditions as considered by simplified methods such as the one proposed by SAP [45–47]. In other words, it is suggested that ICF construction is not performing as other thermally lightweight constructions. The findings from this study support this statement; in order to calculate the U-value with the use of the BS ISO 9869-1:2014 average method all data were considered and the methodology for the heavyweight constructions (with a specific heat capacity per unit area greater than 20 kJ m^{-2} K^{-1}) was adopted as described in Section 2.2. For reasons of consistency in the U-value calculation of the wall elements, the same methodology was used for the first floor SIP walls. On the other hand, the U-value calculation of the glazed elements considered only night-time data. In order to comply with the ISO 9869-1 standard requirements, U-values from heat flux sensors that were installed on areas away from thermal bridges are reported here, i.e. at clear wall areas and centre of pane (in the case of glazing U-values). In total, 16 heat flux sensors were installed in locations away from thermal bridges: 7 on the external walls, 4 on the external windows and 5 on the internal glazed areas.

Similarly to reporting HTC values, the static method (ISO 9869-1) resulted in one U-value for each sensor; the whole testing period was chosen for the analysis in order to increase confidence on the results (as averaging of the heat flows and temperatures would be over a large period of time) and also to obtain the U-values from all sensors over the same averaging period. In most cases the ISO 9869-1 criteria were met within 4 days, while in one case after 7 days of testing (ICF wall). On the other hand, the QUB/e method was able to determine the U-values on a daily basis (i.e., 18 results per sensor were obtained during the dynamic testing period).

4 Results and discussion

4.1 Heat transfer coefficient

The analysis focused on evaluating the ability of the QUB/e method to provide precise and accurate estimates for specific weather and testing conditions. Results reported here are from these tests that successfully met the requirement of maintaining the value of the α-parameter within the recommended limits. A detailed discussion on the influence of the α-parameter on the HTC estimates can be found in [29]. The value of the HTC determined with the coheating test (MLR analysis) will be considered as the reference (benchmark) value to assess the accuracy of the QUB/e method.

4.1.1 Results precision

Figure 7 represents the HTC estimates, noted $\hat{H}$, and their associated 95% confidence intervals, obtained for each QUB/e test. The dashed black lines represent the mean value, the dark grey and grey shaded areas correspond to deviations of ± 10% and ± 20% from the mean value, respectively. Descriptive statistics of the measurements and estimates of the population mean are reported in Table 2.

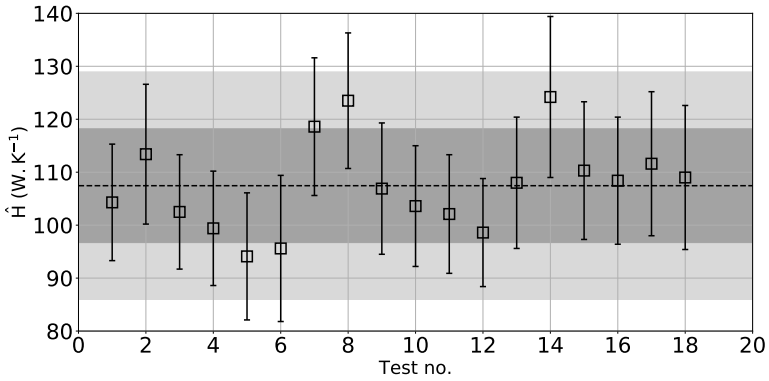

Figure 7: HTC estimates for each QUB/e test. The dashed black line represent the mean value, the dark grey and grey shaded areas correspond to deviations of ± 10% and ± 20% from the mean value, respectively.

No. of tests	**HTC** ($W K^{-1}$)			
	mean	SD (CoV)	SEM	U_{95}
18	107.4	8.4 (7.8%)	2.0	4.3

Table 2: Descriptive statistics of the measurements and estimates of the population mean (SD = Standard Deviation, CoV = Coefficient of Variation, SEM = Standard Error of the Mean, U_{95} = absolute uncertainty of the mean for 95% confidence interval)

The mean HTC, and its associated 95% confidence interval, is 107.4 ± 4.3 $W K^{-1}$ (± 4.0%). All the HTC estimates obtained from the 18 QUB/e tests which fulfilled a value of the α-parameter within the recommended limits lay within ± 20 % of the mean value. More specifically, 13 results were within ± 10% from the mean value and further 4 results were within ± 15%. In total, 94% of the results (i.e. 17 out of 18) were found to be within ± 15% from the mean.

These results were consistent with the findings reported in an uninsulated property [31]. It also suggests that the precision of the QUB/e method is similar regardless of the levels of thermal insulation of the building investigated.

4.1.2 Weather and testing conditions

Robustness of the method in determining the HTC of the building was investigated in terms of the effect of specific testing conditions on the obtained results. In the first long-term study conducted in an uninsulated property [31], it was found that the results obtained were not correlated to common occurring wind and solar conditions. However, the internal starting temperature was found to have an effect on the results due to the

ground floor losses that were not consistent with the losses occurring from the rest of the building envelope that was in contact to the external temperature (ibid). In order to evaluate the performance of the method in a well-insulated property, weather conditions were monitored throughout the testing campaign and the same analysis was performed to assess the potential effect of the testing conditions.

Solar radiation: There was no correlation between the solar irradiance and the resulting HTC since the experimental set-up was deliberately arranged to exclude the direct solar gains transmitted in the internal space throughout the daytime (see Figure 4). The absorbed solar gains through the opaque elements of the building fabric were the only mechanism that would affect the building's energy balance; the effect of these gains on the internal temperature is deemed very small considering the low U-values of the walls and the roof and the fact that these would be diminished by the time the internal slopes are calculated which is several hours after each phase commences.

Wind conditions: Wind conditions are likely to affect the thermal performance of a building mainly through increased infiltration losses. Average wind speeds observed during the testing period were low (the maximum average wind speed observed was approximately $2.5\,\mathrm{m\,s^{-1}}$), while the heated area was sheltered from three sides (nearby buildings sheltering the east and west side of the building while the south facing area was sheltered from the sunspace acting as a buffer zone). Therefore, wind conditions did not affect the results; infiltration losses were mainly stack induced, affected by the difference between the internal and external temperature, rather than wind induced. This was also investigated experimentally. Vega Pasos et al. [34] conducted a constant concentration tracer gas test based on the procedure set by the BS EN ISO 12569:2017 Standard [48] to investigate the infiltration characteristics of the house. The continuous infiltration rate (shortest time interval 3.5 minutes) during a 3-day period (when QUB/e tests were also performed) were calculated and it was found that the infiltration rate, and consequently the infiltration losses of the dwelling, were dominated by the temperature difference between the internal and external environment, while wind resulted only in peaks of the infiltration rate during wind gusts [34].

External temperature: External temperature was found to have a profound effect on test results in the uninsulated property. Higher values of HTC were reported at days with higher external starting temperature. This was attributed to the methodology followed where the internal starting temperature was adjusted to the external one in order to maintain a desirable temperature difference and consequently the value of the α-parameter within the recommended limits (as there was no option to adjust the power input); this led to increased heat losses through the ground and consequently at higher values of HTC [28]. A methodology was proposed to deduct the heat losses from the floor and it was found that the external temperature had no effect on the adjusted HTC [31].

Such effect of the external temperature on the HTC was not found in this case (Figure 8a). This appears to be inconsistent with the findings reported in the uninsulated property [31]. However, in this case the test was conducted differently than it was in the previous case study; both the starting internal temperature and the power input were adjusted to achieve the recommended values of the α-parameter. The relationship between the starting internal temperature and the HTC is shown in Figure 8b. Results are reported separately for tests where the power input was adjusted and tests where the internal temperature was adjusted, in order to achieve a desirable value of the α-parameter. It can be seen that there is no relationship of the HTC with the internal temperature when the power was adjusted while there was very strong correlation when the internal temperature was adjusted (coefficient of determination of 0.8). It should be noted that the house examined has a large surface area that is not in direct contact to the external temperature, i.e. the area of the floor that is in contact to the ground and the area of the internal glazing in contact to the sunspace area. For this reason, adjusting the internal temperature based on the external one may result in increased heat losses on those tests with higher starting internal temperature.

However, this should be treated with care as the number of the tests is not sufficient to draw a definite conclusion. In total, just ten tests were conducted with this adjustment technique (adjusting the starting internal temperature) and only two tests were conducted with markedly higher starting temperature. The correlation between starting internal temperature and the HTC could be the result of a random variation in the HTC in these two tests rather than a systematic overestimation of the HTC. In any case, the starting internal temperature appears to be a factor that needs to be considered when evaluating results of QUB/e tests conducted under varying conditions. Further testing targeting specifically these two adjustments is also suggested. A higher number of tests conducted should provide a more robust indication on whether the starting internal temperature has an impact on the resulting HTC.

It should also be pointed out that due to the fact that the floor was covered with thick carpet it was not possible to establish good thermal contact between the heat flux sensors and the floor in order to obtain reliable

readings. As a result, the method developed to account for the ground losses [31] was not considered applicable in this case.

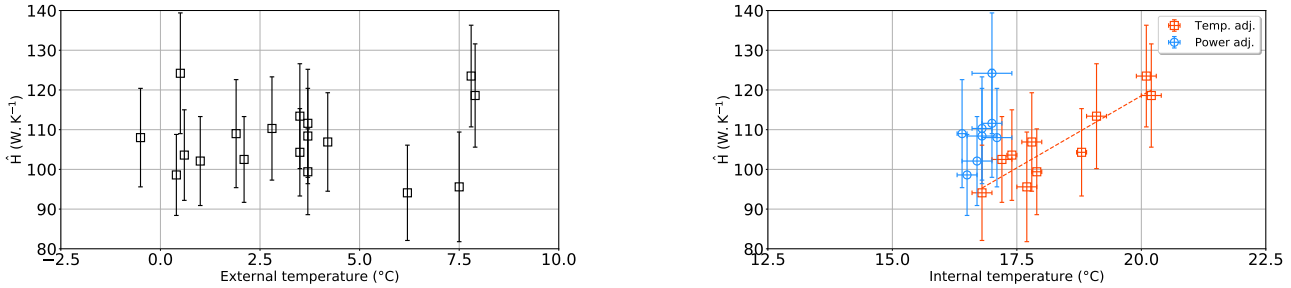

(a) Influence of the starting external temperature

(b) Influence of the starting internal temperature

Figure 8: HTC estimates as a function of the starting external temperature and the starting internal temperature

4.1.3 Results accuracy

Figure 9 represents the HTC estimates, noted $\hat{H}$, and their associated 95% confidence intervals, obtained for each QUB/e test. The dashed line represent the HTC value determined with the coheating test based on the MLR analysis. The shaded area correspond to the 95% confidence interval. If the associated 95% confidence intervals of the HTCs of the different test methods overlap, we cannot detect a statistical difference between them. We observe that all but four (i.e., 14 out of 18 or 78%) HTC estimates obtained with a QUB/e test cannot be considered statistically different from the HTC determined with the coheating test. It should be noted that the reported confidence intervals associated with the HTC estimates obtained with the QUB/e tests are slightly larger than the one reported for the coheating test (i.e., 11.6% in average and 6.1%, respectively). Should the reported confidence intervals of the QUB/e tests be of the same magnitude as the coheating test, four HTC estimates obtained with a QUB/e test could be considered statistically different from the the HTC determined with the coheating test. It is the authors' opinion that it does not undermine the accuracy statement.

The Mean Bias Error (MBE) and the Root Mean Square Error (RMSE) associated with the HTC estimates obtained with the QUB/e tests are $-13.1\,\mathrm{W\,K^{-1}}$ (-10.9%) and $13.9\,\mathrm{W\,K^{-1}}$ (11.5%), respectively. The HTC determined with the coheating test (MLR analysis) was considered as the reference (benchmark) value used to compute the Mean Bias Error (MBE) and the Root Mean Square Error (RMSE). The reported value of the MBE reflects on the underestimation of the HTC estimate with the QUB/e tests. It should be noted that this underestimation was not observed in previous published studies (e.g., at the Salford Energy House in UK [13, 24, 27] and at the IBP Twin Houses in Germany [13]) and will be investigated in further work.

These results demonstrate that the QUB/e method can deliver an accurate HTC estimate for the type of dwelling investigated in this study.

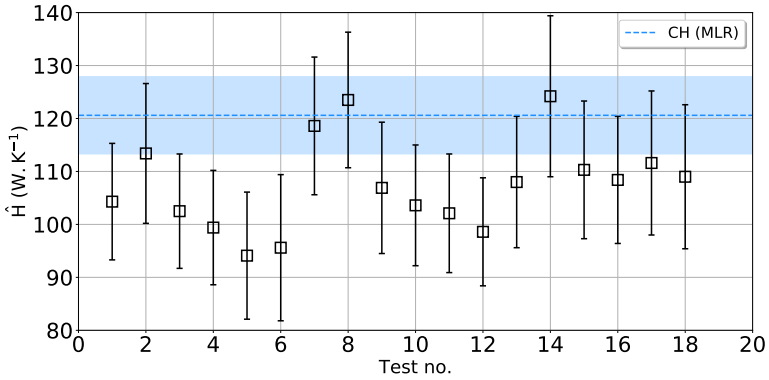

Figure 9: HTC estimates for each QUB/e test. The dashed line and the shaded area represent the HTC value determined with the coheating test based on the MLR analysis and its associated 95% confidence interval, respectively.

4.2 Thermal transmittance of building elements

The analysis focused on evaluating the ability of the QUB/e method to provide precise and accurate estimates of the thermal transmittance of the external walls and the glazings. The values of the thermal transmittances determined with the ISO 9869-1 average method will be considered as the reference (benchmark) values to assess the accuracy of the QUB/e method.

4.2.1 Results precision

Figure 10 and Figure 11 represent the estimates of the U-values, noted $\hat{U}$, and their associated 95% confidence intervals, obtained for each QUB/e test for the external walls (seven different locations) and the glazings (nine different locations), respectively. The dashed black lines represent the mean values, the dark grey and grey shaded areas correspond to deviations of ± 10% and ± 20% from the mean values, respectively. Descriptive statistics of the measurements and estimates of the population means are reported in Table 3 and Table 4.

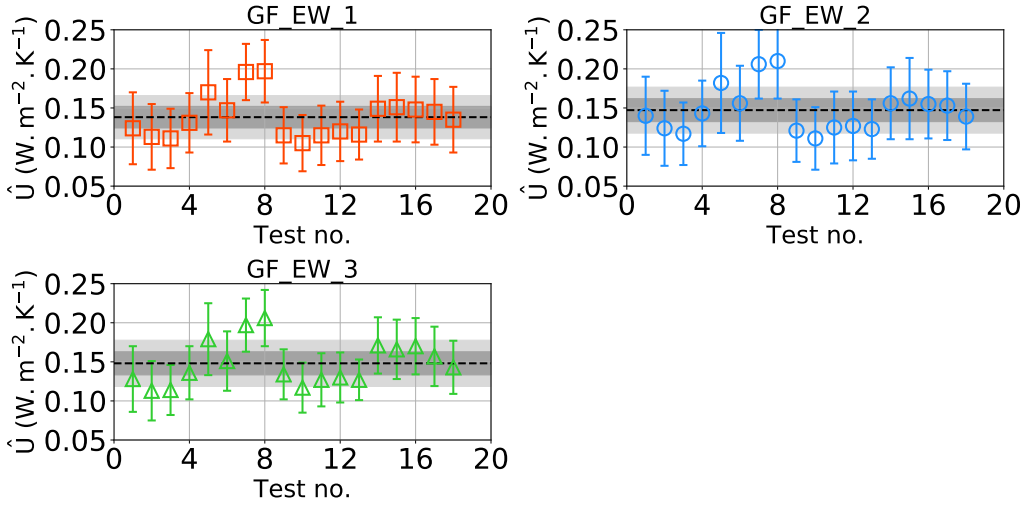

(a) Ground Floor (GF)

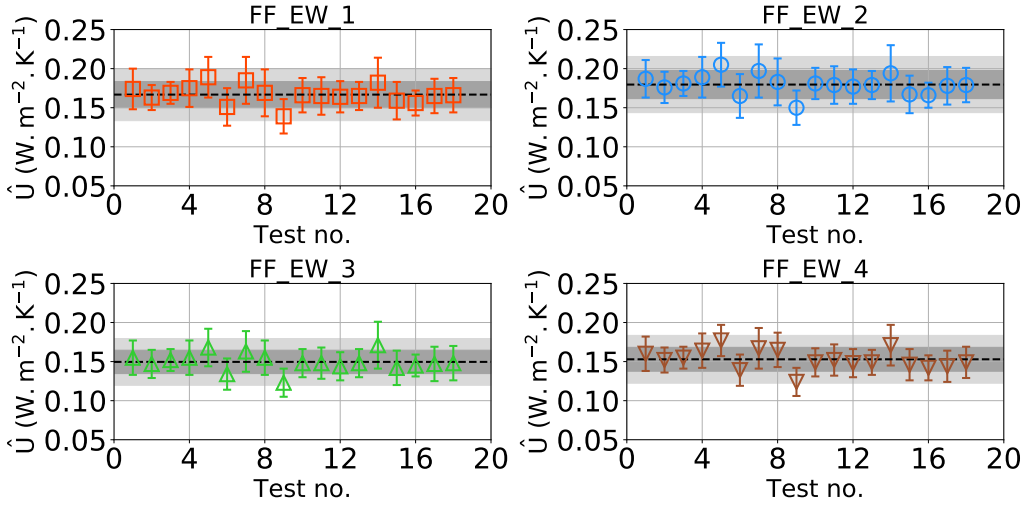

(b) First Floor (FF)

Figure 10: U-values estimates for each QUB/e test for the external walls (7 different locations). The dashed black lines represent the mean values, the dark grey and grey shaded areas correspond to deviations of ± 10% and ± 20% from the mean values, respectively.

We observe two distinct behaviours with regard to the estimates of the U-values of the external walls for the Ground Floor (GF) and the First Floor (FF). The estimates of the U-values of the external walls located on the GF exhibit a large dispersion around their mean values (i.e., the coefficient of variations are approximately 20% for the three different locations investigated here). The observed dispersion is consistent with the relative uncertainty associated with the estimates of each QUB/e test (approximately 29% in average). The estimates

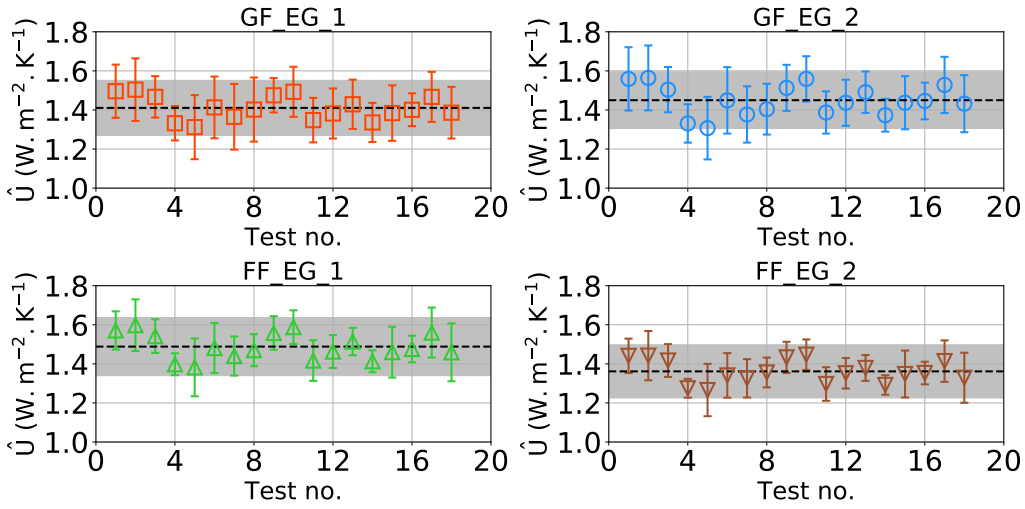

(a) External glazings

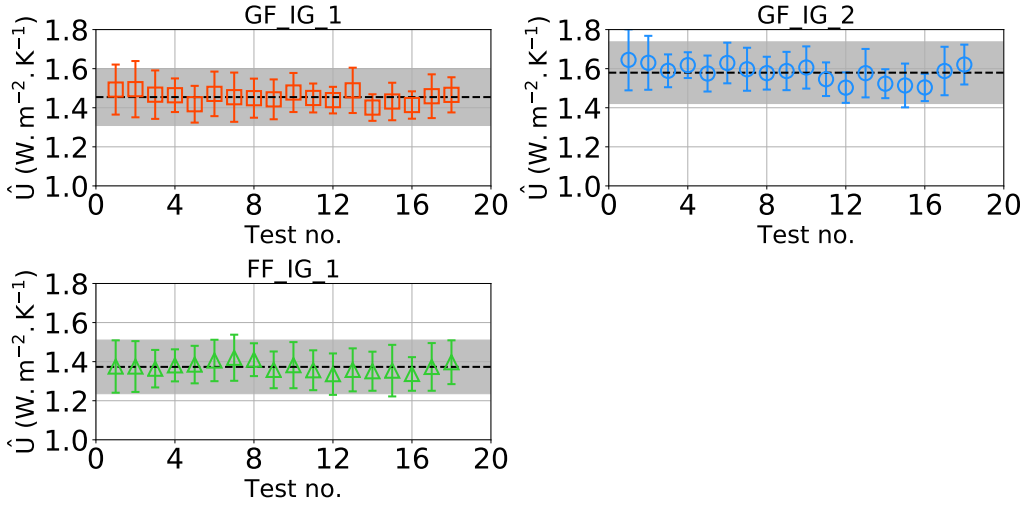

(b) Internal glazings

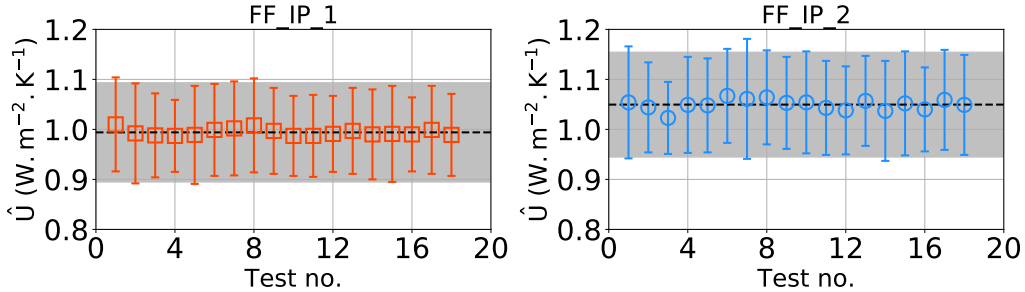

(c) Internal panels

Figure 11: U-values estimates for each QUB/e test for the glazings (9 different locations). The dashed black lines represent the mean values, the dark grey shaded areas correspond to deviations of ± 10% from the mean values.

obtained for the external walls located on the FF are less dispersed around their mean values (i.e., the coefficient of variations are smaller than 7% for the four different locations investigated here). It is believed that the larger dispersion observed on the ICF wall is due to the increased levels of thermal mass of this construction type compared to SIP panels; however, further work is required to verify this.

The distributions of the U-values estimates for the external walls are shown in Figure 12. The boxes represent the 25^{th}, 50^{th} and 75^{th} percentiles of the data and the whiskers extend up to 1.5 times the interquartile range outside the box boundaries. Dots that appear outside the whiskers are considered outliers. There is only one result that statistically appears to be an outlier (ICF wall). The mean U-values, and their associated

Location	**HFP**	**U-value** ($W\,m^{-2}\,K^{-1}$)			
		mean	SD (CoV)	SEM	U_{95}
Ground Floor (GF)	GF_EW_1	0.14	0.03 (19.4%)	0.01	0.01
	GF_EW_2	0.15	0.03 (19.0%)	0.01	0.01
	GF_EW_3	0.15	0.03 (18.5%)	0.01	0.01
First Floor (FF)	FF_EW_1	0.17	0.01 (6.9%)	0.00	0.01
	FF_EW_2	0.18	0.01 (6.9%)	0.00	0.01
	FF_EW_3	0.15	0.01 (7.3%)	0.00	0.01
	FF_EW_4	0.15	0.01 (8.1%)	0.00	0.01

Table 3: U-values estimates of the external walls – Descriptive statistics of the measurements and estimates of the population means (SD = Standard Deviation, CoV = Coefficient of Variation, SEM = Standard Error of the Mean, U_{95} = absolute uncertainty of the mean for 95% confidence interval).

Location	**HFP**	**U-value** ($W\,m^{-2}\,K^{-1}$)			
		mean	SD (CoV)	SEM	U_{95}
External Glazings	GF_EG_1	1.41	0.06 (4.2%)	0.01	0.03
	GF_EG_2	1.45	0.08 (5.2%)	0.02	0.04
	FF_EG_1	1.49	0.07 (4.4%)	0.02	0.03
	FF_EG_2	1.36	0.06 (4.2%)	0.01	0.03
Internal Glazings	GF_IG_1	1.45	0.03 (1.8%)	0.01	0.01
	GF_IG_2	1.58	0.04 (2.7%)	0.01	0.02
	FF_IG_1	1.37	0.02 (1.7%)	0.01	0.01
Internal Panels	FF_IP_1	0.99	0.01 (0.7%)	0.00	0.00
	FF_IP_2	1.05	0.01 (1.0%)	0.00	0.01

Table 4: U-values estimates of the glazings – Descriptive statistics of the measurements and estimates of the population means (SD = Standard Deviation, CoV = Coefficient of Variation, SEM = Standard Error of the Mean, U_{95} = absolute uncertainty of the mean for 95% confidence interval).

95% confidence intervals, are $0.14 \pm 0.03\,W\,m^{-2}\,K^{-1}$ ($\pm$ 5.3%) and $0.16 \pm 0.00\,W\,m^{-2}\,K^{-1}$ ($\pm$ 2.5%) for the external walls located on the GF and the FF, respectively. These values are consistent with the design value of $0.15\,W\,m^{-2}\,K^{-1}$.

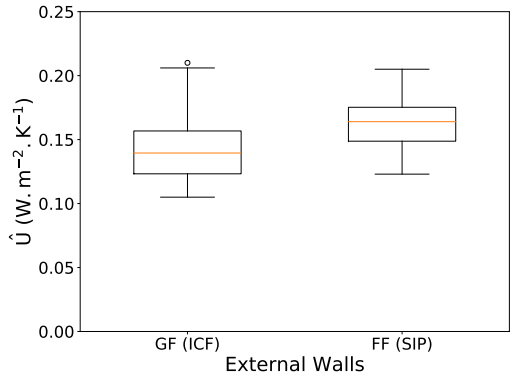

Figure 12: Box plot of the U-values estimates for the external walls (GF = Ground Floor, FF = First Floor).

The estimates of the U-values of the glazings show a relatively small dispersion around their mean values (i.e., their coefficient of variations are smaller than 5%).

The distributions of the U-values estimates for the external walls are shown in Figure 13. The mean U-values, and their associated 95% confidence intervals, are $1.43 \pm 0.02\,W\,m^{-2}\,K^{-1}$ ($\pm$ 1.3%), $1.47 \pm 0.02\,W\,m^{-2}\,K^{-1}$ ($\pm$ 1.7%) and $1.02 \pm 0.01\,W\,m^{-2}\,K^{-1}$ ($\pm$ 1.0%) for the external glazings, the internal glazings and the internal

panels, respectively. These values are consistent with the design value of 1.66 and 1.70 $\mathrm{W\,m^{-2}\,K^{-1}}$ for the external (north façade) windows and the internal (south façade) windows (the centre pane values were not available).

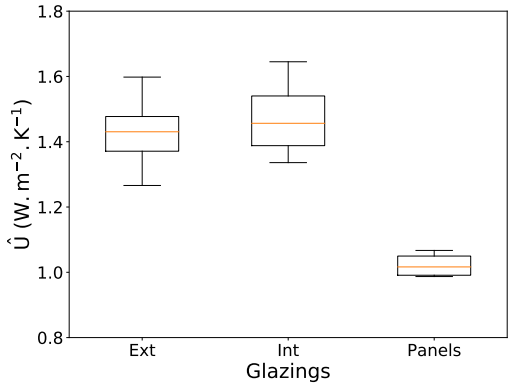

Figure 13: Box plot of the U-values estimates for the glazings.

4.2.2 Results accuracy

Figure 14 and Figure 15 represent the U-values estimates, noted $\hat{U}$, and their associated 95% confidence intervals, obtained for each QUB/e test for the external walls (seven different locations) and the glazings (nine different locations), respectively. The dashed lines represent the U-values determined with the ISO 9869-1 average method. The shaded areas correspond to the 95% confidence intervals. If the associated 95% confidence intervals of the U-values of the different test methods overlap, we cannot detect a statistical difference between them.

We observe that all but seven (i.e., 119 out of 126 or 94%) U-values estimates of the external walls obtained with a QUB/e test cannot be considered statistically different from the U-values determined with the ISO 9869-1 average method. With regard to the glazings, this is observed for all U-values estimates (i.e., 162 out of 162 or 100%). It should be noted that the reported confidence intervals associated with the U-value estimates obtained with both test methods are close (i.e., approximately 10% in average) for all elements except for the ICF wall (i.e., approximately 29% and 10% in average for the QUB/e method and the ISO 9869-1 average method, respectively).

The U-values determined with both the ISO 9869-1 and QUB/e methods for the external walls and the glazings are reported in Table 5 and Table 6, respectively. The values reported for the QUB/e method are the mean U-values, and their associated 95% confidence intervals. The U-value determined with the ISO 9869-1 average method was considered as the reference (benchmark) value used to compute the Mean Bias Error (MBE) and the Root Mean Square Error (RMSE).

The mean values of the MBE and the RMSE associated with the U-values estimates obtained with the QUB/e tests are $-0.02\,\mathrm{W\,m^{-2}\,K^{-1}}$ (-11.9%) and $0.03\,\mathrm{W\,m^{-2}\,K^{-1}}$ (18.2%) for the ICF wall (GF) and $0.01\,\mathrm{W\,m^{-2}\,K^{-1}}$ (10.0%) and $0.02\,\mathrm{W\,m^{-2}\,K^{-1}}$ (11.9%) for the SIP wall (FF), respectively. The mean values of the MBE and the RMSE obtained for the glazings are of the same order of magnitude in absolute values but much lower in relative values due to the larger U-values of the glazings. It should also be noted that there does not appear a systematic overestimation or underestimation of U-values (i.e., no bias) when using the QUB/e method.

These results are consistent with the findings of previous studies (e.g., see [24,30]) and demonstrate that the QUB/e method can deliver accurate U-values estimates for the type of external walls and glazings investigated in this study.

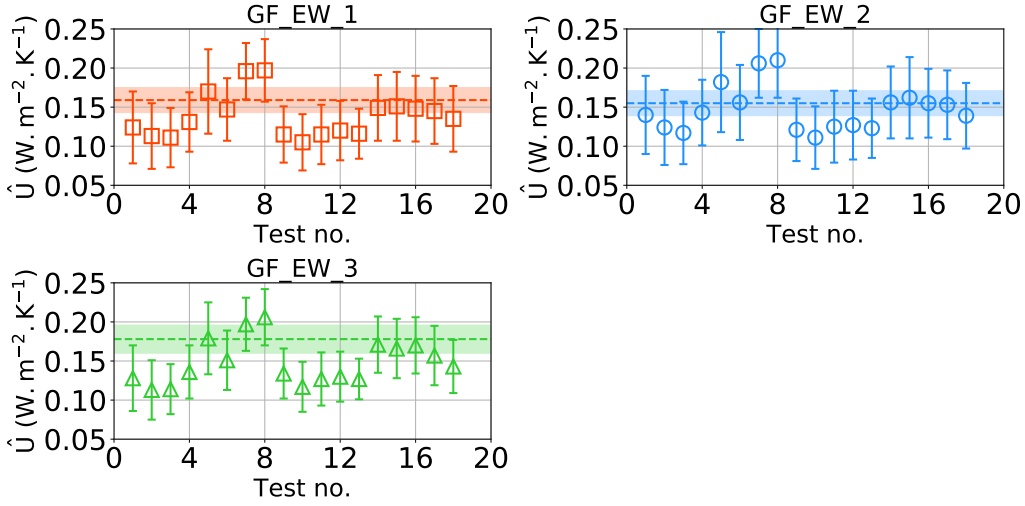

(a) Ground Floor (GF)

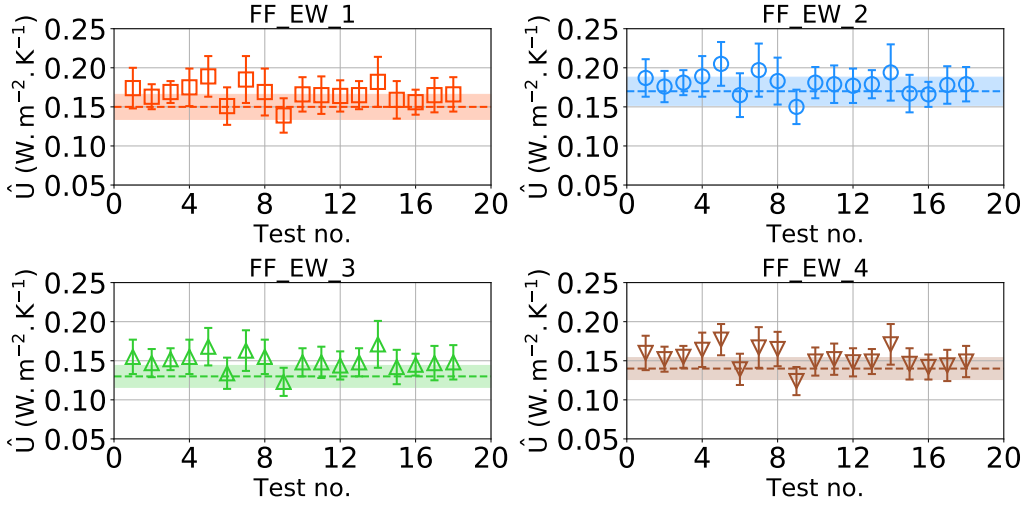

(b) First Floor (FF)

Figure 14: U-values estimates for each QUB/e test for the external walls (7 different locations). The dashed lines and the shaded areas represent the U-values determined with the ISO 9869-1 average method and their associated 95% confidence intervals, respectively.

Location	**HFP**	**U-value** ($W\,m^{-2}\,K^{-1}$)			
		ISO 9869-1	QUB/e	MBE	RMSE
Ground Floor (GF)	GF_EW_1	0.16 ± 0.02 (± 10.1%)	0.14 ± 0.01 (± 9.9%)	-0.02 (-13.1%)	0.03 (19.1%)
	GF_EW_2	0.15 ± 0.02 (± 10.3%)	0.15 ± 0.01 (± 9.7%)	-0.01 (-5.0%)	0.02 (15.2%)
	GF_EW_3	0.18 ± 0.02 (± 10.1%)	0.15 ± 0.01 (± 9.4%)	-0.03 (-16.8%)	0.04 (19.8%)
First Floor (FF)	FF_EW_1	0.15 ± 0.02 (± 10.7%)	0.17 ± 0.01 (± 3.5%)	0.02 (11.2%)	0.02 (12.0%)
	FF_EW_2	0.17 ± 0.02 (± 10.6%)	0.18 ± 0.01 (± 3.5%)	0.01 (5.7%)	0.01 (7.7%)
	FF_EW_3	0.13 ± 0.01 (± 10.8%)	0.15 ± 0.01 (± 3.7%)	0.02 (15.1%)	0.02 (15.7%)
	FF_EW_4	0.14 ± 0.01 (± 10.0%)	0.15 ± 0.01 (± 4.1%)	0.01 (9.2%)	0.01 (10.6%)

Table 5: Comparison of the U-values determined with both the ISO 9869-1 and QUB/e methods for the external walls (MBE = Mean Bias Error, RMSE = Root Mean Square Error).

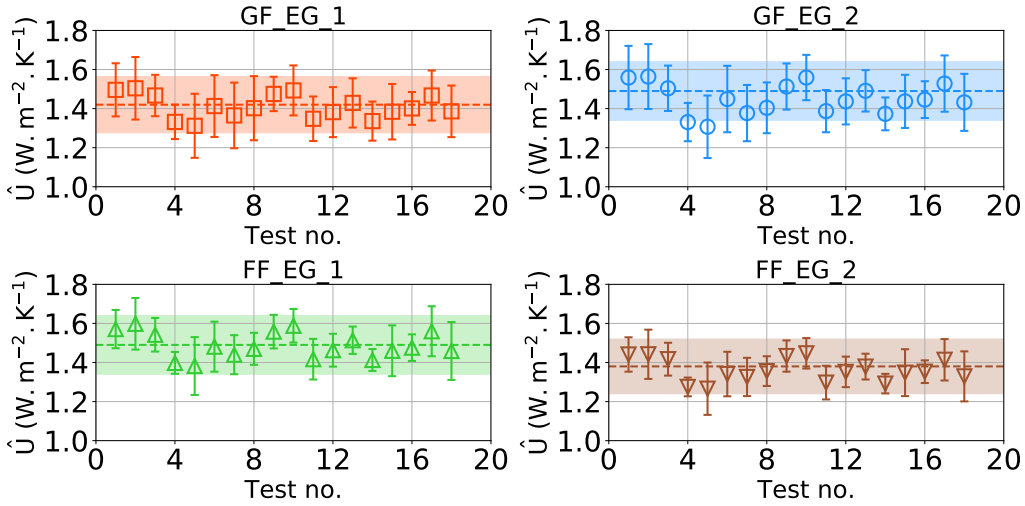

(a) External glazings

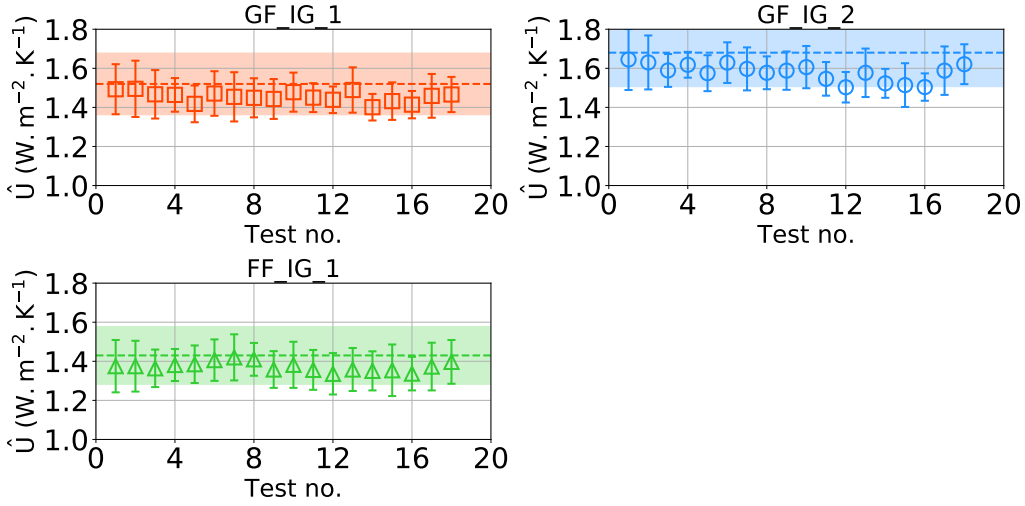

(b) Internal glazings

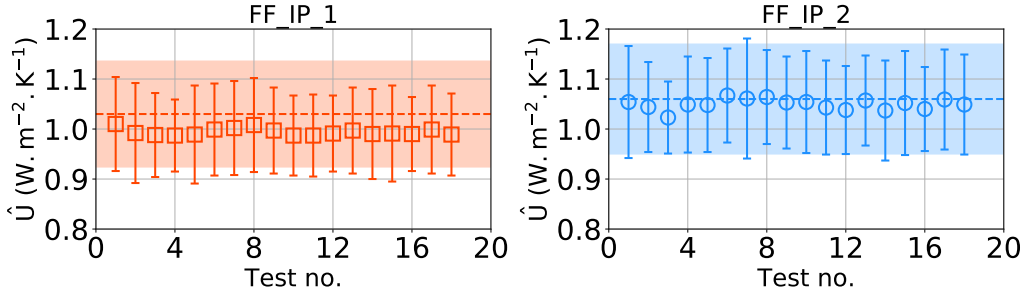

(c) Internal panels

Figure 15: U-values estimates for each QUB/e test for the glazings (9 different locations). The dashed lines and the shaded areas represent the U-values determined with the ISO 9869-1 average method and their associated 95% confidence intervals, respectively.

Location	**HFP**	**U-value** ($W\,m^{-2}\,K^{-1}$)			
		ISO 9869-1	QUB/e	MBE	RMSE
External Glazings	GF_EG_1	1.42 ± 0.14 (± 10.1%)	1.41 ± 0.03 (± 2.1%)	-0.01 (-0.7%)	0.05 (3.7%)
	GF_EG_2	1.49 ± 0.15 (± 10.1%)	1.45 ± 0.04 (± 2.7%)	-0.04 (-2.7%)	0.07 (4.8%)
	FF_EG_1	1.49 ± 0.15 (± 10.1%)	1.49 ± 0.03 (± 2.2%)	-0.00 (-0.1%)	0.06 (3.8%)
	FF_EG_2	1.38 ± 0.14 (± 10.1%)	1.36 ± 0.03 (± 2.2%)	-0.02 (-1.3%)	0.05 (3.9%)
Internal Glazings	GF_IG_1	1.52 ± 0.16 (± 10.4%)	1.45 ± 0.01 (± 0.9%)	-0.07 (-4.3%)	0.07 (4.3%)
	GF_IG_2	1.68 ± 0.17 (± 10.4%)	1.58 ± 0.02 (± 1.4%)	-0.10 (-6.0%)	0.10 (6.0%)
	FF_IG_1	1.43 ± 0.15 (± 10.3%)	1.37 ± 0.01 (± 0.9%)	-0.06 (-4.0%)	0.06 (4.0%)
Internal Panels	FF_IP_1	1.03 ± 0.11 (± 10.3%)	0.99 ± 0.00 (± 0.4%)	-0.04 (-3.5%)	0.04 (3.5%)
	FF_IP_2	1.06 ± 0.11 (± 10.4%)	1.05 ± 0.01 (± 0.5%)	-0.01 (-1.0%)	0.01 (1.1%)

Table 6: Comparison of the U-values determined with both the ISO 9869-1 and QUB/e methods for the glazings (MBE = Mean Bias Error, RMSE = Root Mean Square Error).

5 Conclusions

The findings from a field study conducted to assess the precision and accuracy of the QUB/e method in a well-insulated detached dwelling under UK climate conditions were presented and discussed in this paper. The following conclusions were drawn from the analysis:

1. The QUB/e method was able to provide precise estimates of the whole building HTC. In total, 94% of the results (i.e. 17 out of 18) were found to be within ± 15% from the mean.
2. The QUB/e method was able to provide accurate estimates of the whole building HTC. We observed that 78% of the HTC estimates (i.e., 14 out of 18) obtained with a QUB/e test could not be considered statistically different from the HTC determined with the coheating test (benchmark). It should be noted that the reported confidence intervals associated with the HTC estimates obtained with the QUB/e tests were slightly larger than the one reported for the coheating test (i.e., 11.6% in average and 6.1%, respectively). Besides, the Mean Bias Error (MBE) and the Root Mean Square Error (RMSE) associated with the HTC estimates obtained with the QUB/e tests were approximately 11%.
3. The QUB/e method was also able to provide precise and accurate estimates of the thermal transmittances of the external walls and the glazings. We observed that all but seven (i.e., 119 out of 126 or 94%) U-values estimates of the external walls obtained with a QUB/e test could not be considered statistically different from the U-values determined with the ISO 9869-1 average method (benchmark). With regard to the glazings, this was observed for all U-values estimates (i.e., 162 out of 162 or 100%). It should be noted that the reported confidence intervals associated with the U-value estimates obtained with both test methods were close (i.e., approximately 10% in average) for all elements except for the ICF wall.

The findings of this field study in a well-insulated property in the UK support previous evidence (e.g., see [13, 24, 30, 31]) and increase confidence on the ability of the QUB/e method to provide precise and accurate results in the field.

Furthermore, the QUB/e method was found to be robust as the weather conditions were not found to impact the test results in the building investigated. However, testing conditions may have an impact on the resulting HTC; it has been found that the starting temperature is a parameter that requires further investigation. In addition, similar studies in buildings that are more representative of the current building stock in the UK will be useful for the wider verification of the results and the broader acceptance of the method by researchers and building performance practitioners.

Acknowledgements

The authors gratefully acknowledge funding received from Saint-Gobain and Innovate UK under the KTP009930 project.

References

[1] DBEIS (2020). *Digest of United Kingdom Energy Statistics (DUKES) – Energy: Chapter 1*. Department for Business, Energy and Industrial Strategy.

[2] P. de Wilde (2014). The gap between predicted and measured energy performance of buildings: A framework for investigation. *Automation in Construction*, vol. 41, pp. 40–49. http://dx.doi.org/10.1016/j.autcon.2014.02.009

[3] D. Johnston, D. Miles-Shenton and D. Farmer. Quantifying the domestic building fabric 'performance gap'. *Building Services Engineering Research and Technology*, vol. 36, issue 5, pp. 614–627. https://doi.org/10.1177/0143624415570344

[4] R. Gupta and A. Kotopouleas (2018). Magnitude and extent of building fabric thermal performance gap in UK low energy housing. *Applied Energy*, vol. 222, pp. 673–686. https://doi.org/10.1016/j.apenergy.2018.03.096

[5] Cutland Consulting Limited (2012). *Low and Zero Carbon Homes: Understanding the Performance Challenge*. NHBC Foundation and IHS BRE Press, Watford, UK.

[6] Zero Carbon Hub (2014). *Closing the Gap Between Design and As-built Performance – Evidence Review Report*. London, UK.

[7] BSI (2017). BS EN ISO 13789:2017. *Thermal performance of buildings. Transmission and ventilation heat transfer coefficients. Calculation method*. British Standards Institution (BSI), London, UK.

[8] DECC (2014). *The Government's Standard Assessment Procedure for Energy rating of Dwellings*, 2012 edition. BRE, Garston, UK.

[9] R.C. Sonderegger and M.P. Modera (1979). Electric co-heating: A method for evaluating seasonal heating efficiencies and heat loss rates in dwellings. In: *Proceedings of the Second International CIB Symposium, Energy Conservation in the Built Environment*, Copenhagen, Denmark, May 28 – June 1, 1979.

[10] R.C. Sonderegger, P.E. Condon and M.P. Modera (1980). In-situ measurements of residential energy performance using electric co-heating. In: *American Society of Heating, Refrigeration, and Air-Conditioning Engineers (ASHRAE) semi-annual meeting*, Los Angeles, CA, USA, February 3, 1980. https://www.osti.gov/biblio/5492967

[11] M.F. Fels (1986). PRISM: An introduction. *Energy and Buildings*, vol. 9, issues 1–2, pp. 5–18. https://doi.org/10.1016/0378-7788(86)90003-4

[12] K. Subbarao (1988). *PSTAR: Primary and Secondary Terms Analysis and Renormalization: A Unified Approach to Building Energy Simulations and Short-term Monitoring*. Solar Energy Research Institute, Golden, CO, US.

[13] F. Alzetto, G. Pandraud, R. Fitton, I. Heusler and H. Sinnebichler (2018). QUB: a fast dynamic method for in-situ measurement of the whole building heat loss. *Energy and Buildings*, vol. 174, pp 124–133. https://doi.org/10.1016/j.enbuild.2018.06.002

[14] S. Thébault and R. Bouchié (2018). Refinement of the ISABELE method regarding uncertainty quantification and thermal dynamics modelling. *Energy and Buildings*, vol. 178, pp. 182–205. https://doi.org/10.1016/j.enbuild.2018.08.047

[15] D. Johnston, D. Miles-Shenton, D. Farmer and J. Wingfield (2013). *Whole House Heat Loss Test Method (Coheating)*. Leeds Metropolitan University, Leeds, UK.

[16] BSI (2014). BS ISO 9869-1:2014. *Thermal insulation – Building elements – In situ measurement of thermal resistance and thermal transmittance – Part 1: Heat flow meter method*. British Standards Institution (BSI), London, UK.

[17] GHA (2011). *GHA Monitoring Programme 2009-11: Technical Report, Results from Phase 1: Post-construction testing of a sample of highly sustainable new homes*. Good Homes Alliance, London, UK.

[18] A. Janssens (2016). *Overview of Methods to Analyse Dynamic Data. International Energy Agency, EBC Annex 58, Reliable building energy performance characterisation based on full scale dynamic measurements*. KU Leuven, Leuven, Belgium.

[19] S. Rouchier, M.J. Jiménez and S. Castao (2019). Sequential Monte Carlo for on-line parameter estimation of a lumped building energy model. *Energy and Buildings*, vol. 187, pp 86–94. https://doi.org/10.1016/j.enbuild.2019.01.045

[20] M. Senave, S. Roels, G. Reynders, S. Verbeke and D. Saelens (2020). Assessment of data analysis methods to identify the heat loss coefficient from on-board monitoring data. *Energy and Buildings*, vol. 209, art. no. 109706. https://doi.org/10.1016/j.enbuild.2019.109706

[21] N. Soares, C. Martins, M. Goncalves, P. Santos, L. Simoes Da Silva, and K.J. Costa (2019). Laboratory and in-situ non-destructive methods to evaluate the thermal transmittance and behavior of walls, windows, and construction elements with innovative materials: A review. *Energy and Buildings*, vol. 182, pp. 88–110. https://doi.org/10.1016/j.enbuild.2018.10.021

[22] D. Bienvenido-Huertas, J. Moyano, D Marin, and R. Fresco-Contreras (2019). Review of in situ methods for assessing the thermal transmittance of walls. *Renewable and Sustainable Energy Reviews*, vol. 102, pp. 356–371. https://doi.org/10.1016/j.rser.2018.12.016

[23] M. Teni, H. Krstić, and P. Kosiński (2019). Review and comparison of current experimental approaches for in-situ measurements of building walls thermal transmittance. *Energy and Buildings*, vol. 203, art. no. 109417. https://doi.org/10.1016/j.enbuild.2019.109417

[24] J. Meulemans, F. Alzetto, D. Farmer and C. Gorse (2017). QUB/e A novel transient experimental method for in situ measurements of the thermal performance of building fabrics. In: Gorse, C. and Dastbaz, M. (eds), *Building Information Modelling, Building Performance, Design and Smart Construction*, Springer, Cham, Switzerland. https://doi.org/10.1007/978-3-319-50346-2_9

[25] C. Ghiaus and F. Alzetto (2019). Design of experiments for Quick U-building (QUB) method for building energy performance measurement. *Journal of Building Performance Simulation*, vol. 12 (4), pp 465–479. https://doi.org/10.1080/19401493.2018.1561753

[26] N. Ahmad, C. Ghiaus and T. Thiery (2020). Influence of Initial and Boundary Conditions on the Accuracy of the QUB Method to Determine the Overall Heat Loss Coefficient of a Building. *Energies*, vol. 13, issue 1, p. 284. https://doi.org/10.3390/en13010284

[27] F. Alzetto, D. Farmer, R. Fitton, T. Hughes and W. Swan (2018). Comparison of whole house heat loss test methods under controlled conditions in six distinct retrofit scenarios. *Energy and Buildings*, vol. 168, pp. 35–41. https://doi.org/10.1016/j.enbuild.2018.03.024

[28] V. Sougkakis, J. Meulemans, F. Alzetto, C. Wood, M. Gillott and T. Cox (2017). An assessment of the QUB method for predicting the whole building thermal performance under actual operating conditions. In: Gorse, C. (Ed.) *International Sustainable Ecological Engineering Design for Society (SEEDS) Conference 2017 – Conference Proceedings*, 13 – 14 September 2017, Leeds, UK. Leeds Beckett University, Leeds, UK. https://hal.archives-ouvertes.fr/hal-01589204

[29] V. Sougkakis, J. Meulemans, C. Wood, M. Gillott and T. Cox (2018). QUB/e: Validation of a transient method for determining whole building thermal performance and building element U-values in situ under actual operating conditions. In S. Riffat, Y. Su, D. Liu, and Y. Zhang, editors, *The 17th International Conference on Sustainable Energy Technologies – SET 2018*, volume 3, pp. 174–184, 21 – 23 August 2018, Wuhan, China. University of Nottingham, Nottingham, UK. https://nottingham-repository.worktribe.com/output/1607959

[30] J. Meulemans (2019). An assessment of the QUB/e method for fast in situ measurements of the thermal performance of building fabrics in cold climates. In: Johansson D., Bagge H., Wahlström Å. (eds) *Cold Climate HVAC 2018, Springer Proceedings in Energy*. Springer, Cham, Switzerland. https://doi.org/10.1007/978-3-030-00662-4_27

[31] V. Sougkakis, J. Meulemans, C. Wood, M. Gillott and T. Cox (2021). Field testing of the QUB method for assessing the thermal performance of dwellings: in situ measurements of the heat transfer coefficient of a circa 1950s detached house in UK. *Energy and Buildings*, vol. 230, art. 110540, 2021. https://doi.org/10.1016/j.enbuild.2020.110540

[32] DECC (2008). The Code for Sustainable Homes – Setting the standard in sustainability for new homes. Wetherby: Communities and Local Government Publications. Department of Energy and Climate Change, London, UK.

[33] https://www.nottingham.ac.uk/creative-energy-homes/houses/basf-research-house/basf-research-house.aspx (last access: March 23, 2021)

[34] A. Vega Pasos (2020). *Air infiltration modelling based on low-pressure airtightness measurements*. PhD thesis, University of Nottingham, Nottingham, UK.

[35] L. Rodrigues (2009). *An investigation into the use of thermal mass to improve comfort in British Housing*. PhD thesis, The University of Nottingham, Nottingham, UK.

[36] S. Stamp (2015). *Assessing Uncertainty in co-heating tests: Calibrating a whole building steady state heat loss measurement method*. PhD thesis, University College London, London, UK.

[37] G. Bauwens and S. Roels (2014). Co-heating test: A state-of-the-art. *Energy and Buildings*, vol. 82, pp. 163 – 172. https://doi.org/10.1016/j.enbuild.2014.04.039

[38] R. Jack (2015). *Building Diagnostics: Practical Measurement of the Fabric Thermal Performance of Houses*. PhD Thesis, Loughborough University, Loughborough, UK.

[39] R. Jack, D. Loveday, D. Allinson and K. Lomas (2017). First evidence for the reliability of building co-heating tests. *Building Research & Information*, vol. 46, issue 4, pp. 383–401. https://doi.org/10.1080/09613218.2017.1299523

[40] A. Stafford, D. Johnston, D. Miles-Shenton, D. Farmer, M. Brooke-Peat, and C. Gorse (2014). Adding value and meaning to coheating tests. *Structural Survey*, vol. 32, issue 4, pp. 331–42. https://doi.org/10.1108/SS-01-2014-0007

[41] H.W. Coleman and G.W. Steele (2009). *Experimentation, Validation, and Uncertainty Analysis for Engineers*. John Wiley & Sons, Inc., Hoboken, New Jersey.

[42] D. Butler and A. Dengel (2013). *Review of co-heating test methodologies*. National House Building Council (NHBC) Foundation, Milton Keynes, UK.

[43] R. Everett, A. Horton and J. Doggart (1985). *Linford Low Energy Houses*. Energy Research Group, Open University, Milton Keynes, UK.

[44] P. Baker (2015). *A retrofit of a Victorian terrace house in New Bolsover: A whole house thermal performance assessment*. Historic England & Glasgow Caledonian University, Glasgow, Scotland, UK.

[45] E. Mantesi, C.J. Hopfe, M.J. Cook, J. Glass, and P. Strachan (2018). The modelling gap: quantifying the discrepancy in the representation of thermal mass in building simulation. *Building and Environment*, vol. 131, pp. 74 – 98, https://doi.org/10.1016/j.buildenv.2017.12.017

[46] E. Mantesi, C.J. Hopfe, K. Mourkos, J. Glass and M. Cook (2019). Empirical and computational evidence for thermal mass assessment: The example of insulating concrete formwork. *Energy and Buildings*, vol. 188–189, pp. 314–332. https://doi.org/10.1016/j.enbuild.2019.02.021

[47] H.H. Saber, W. Maref, M. Armstrong, M.C. Swinton, M.Z. Rousseau, G. Gnanamurugan (2011). Numerical Simulations to Predict the Thermal Response of Insulating Concrete Form (ICF) Wall in Cold Climate. Research Report RR-310, National Research Council of Canada, Ottawa, Ontario, Canada.

[48] BSI (2017). BS EN ISO 12569:2017. *Thermal performance of buildings and materials – Determination of specific airflow rate in buildings – Tracer gas dilution method*. British Standards Institution (BSI), London, UK.